PROCEEDINGS OF SCIENCE

Dynamical Structure of Baryons

A. Aleksejevs*
Grenfell Campus of Memorial University
E-mail: aaleksejevs@grenfell.mun.ca

S. Barkanova
Acadia University
E-mail: svetlana.barkanova@acadiau.ca

Compton scattering offers a unique opportunity to study the dynamical structure of hadrons over a wide kinematic range, with polarizabilities characterizing the hadron's active internal degrees of freedom. We present calculations and detailed analysis of the electric, magnetic, and spin-dependent dynamical polarizabilities for the lowest in mass SU(3) octet of baryons. These extensive calculations are made possible by the recent implementation of semi-automatized calculations in chiral perturbation theory which allows evaluating polarizabilities from Compton scattering up to next-to-the-leading order. The dependencies for the range of photon energies covering the majority of the meson photoproduction channels are analyzed.

36th International Conference on High Energy Physics,
July 4-11, 2012
Melbourne, Australia

*Speaker.

PoS(ICHEP2012)469

1. Introduction

One of the major goals of low-energy QCD is the investigation of the baryon response to the external electromagnetic field via a multipole excitation mechanism. Structure parameters which describe that response are electric, magnetic and spin-dependent polarizabilities. In other words, the polarizabilities are related to the deformability and stiffness of the baryon. A precise determination of nucleon polarizabilities still requires substantial effort from both theory and experiment. For hyperons, the polarizabilities are yet to be measured. In this work, we study the polarizabilities of baryons using the Compton scattering, which is a straightforward process from both theoretical and experimental points of view. In general, the polarizabilities in a very low energy region of the Compton scattering are treated as static (with very little or no dependence on the photon energy), but it can be assumed that at higher energies, and especially near meson production threshold, this static behavior will break and the polarizabilities will become dynamic. The main goal of this work is a study of dependence of the electric, magnetic and spin-dependent polarizabilities on the photon energy. We use the relativistic chiral perturbation theory (ChPTh) while applying the multipole expansion approach for the Compton structure functions. The various versions of ChPTh predict a rather broad spectrum of values for polarizabilities, but to date it is the only theory available in the regime of non-perturbative QCD and has been employed here using our computational hadronic model (CHM [5]). CHM gives us a possibility to avoid the low-energy approximation in the Compton structure functions and retain all the possible degrees of freedom arising from SU(3) chiral Lagrangian. We provide a short description of the formalism used in this work in the section "Formalism". Analysis of the dynamical behavior of polarizabilities along with their static values is presented in the "Results".

2. Formalism

In the presence of an external electromagnetic field, induced electric and magnetic dipole moments of the baryon generate effective Hamiltonian $H_{eff} = -\frac{1}{2}4\pi\alpha\mathbf{E}^2 - \frac{1}{2}4\pi\beta\mathbf{H}^2$. Here, proportionality constants α and β are called electric and magnetic polarizabilities, respectively. Although the polarizability values are quite small ($10^{-4}\,(fm^3)$), they were successfully measured by several experimental groups using the Compton scattering and employing the dispersion sum rules analysis to extract the polarizabilities from the cross section data. The current PDG [1] averaged experimental values for the electric and magnetic polarizabilities for protons and neutrons are:

$$\alpha_p = (12.0 \pm 0.6)10^{-4}(fm^3); \quad \beta_p = (1.9 \pm 0.5)10^{-4}(fm^3);$$
$$\alpha_n = (11.6 \pm 1.5)10^{-4}(fm^3); \quad \beta_n = (3.7 \pm 2.0)10^{-4}(fm^3).$$

For protons and neutrons α and β values are approximately the same, and the positive value of the magnetic polarizability points to the paramagnetic nature of the nucleon.

If the baryon is placed in the time-varying electromagnetic field, another set of dipole moments is induced and the following effective Hamiltonianl describes that type of interaction:

$$H_{eff}^{spin} = -\tfrac{1}{2}2\pi\gamma_{E1E1}\boldsymbol{\sigma}\cdot(\mathbf{E}\times\dot{\mathbf{E}}) - \tfrac{1}{2}2\pi\gamma_{M1M1}\boldsymbol{\sigma}\cdot(\mathbf{B}\times\dot{\mathbf{B}}) - 4\pi\gamma_{M1E2}\sigma_i B_j E_{ij} - 4\pi\gamma_{E1M2}\sigma_i E_j B_{ij} \tag{2.1}$$

$$T_{ij} = \tfrac{1}{2}(\partial_i T_j + \partial_j T_i); \ \mathbf{T} = \{\mathbf{E}, \mathbf{B}\}.$$

The coefficients of the proportionality in the Eq.(2.1), γ_{E1E1}, γ_{M1M1}, γ_{M1E2} and γ_{E1M2} are called spin-dependent polarizabilities and correspond to the dipole-dipole and dipole-quadrupole electric/magnetic transitions. It is quite difficult to measure these spin-dependent polarizabilities separately, but for the specific kinematics of the forward/backward scattering these structure parameters can be combined into so-called forward γ_0 and backward γ_π polarizabilities, $\gamma_0 = -\gamma_{E1E1} - \gamma_{M1M1} - \gamma_{M1E2} - \gamma_{E1M2}$ and $\gamma_\pi = -\gamma_{E1E1} + \gamma_{M1M1} + \gamma_{M1E2} - \gamma_{E1M2}$, and can be accessed by the experiment. In order to evaluate the polarizabilities theoretically, one can use the Compton scattering and relate the amplitude to the set of the Compton structure functions R_i [3] in the following way:

$$\begin{aligned}\tfrac{1}{8\pi W}M(\gamma B \to \gamma' B) = {} & R_1(\varepsilon'^{*}\cdot\varepsilon) + R_2(\mathbf{s}'^{*}\cdot\mathbf{s}) + iR_3\sigma\cdot(\varepsilon'^{*}\times\varepsilon) + iR_4\sigma\cdot(\mathbf{s}'^{*}\times\mathbf{s}) + \\ & iR_5((\sigma\cdot\hat{\mathbf{k}})(\mathbf{s}'^{*}\cdot\varepsilon) - (\sigma\cdot\hat{\mathbf{k}}')(\mathbf{s}\cdot\varepsilon'^{*})) + iR_6((\sigma\cdot\hat{\mathbf{k}}')(\mathbf{s}'^{*}\cdot\varepsilon) - (\sigma\cdot\hat{\mathbf{k}})(\mathbf{s}\cdot\varepsilon'^{*}))\end{aligned} \tag{2.2}$$

Here, $W = \omega + \sqrt{\omega^2 + m_B^2}$ is the center of mass energy and ω is the energy of the incoming photon. The unit magnetic vector ($\mathbf{s} = (\hat{\mathbf{k}} \times \varepsilon)$), polarization vector ($\varepsilon$) and unit momentum of the photon ($\hat{\mathbf{k}} = \dfrac{\mathbf{k}}{k}$) are denoted by the prime for the case of the outgoing photon. Although the choice of the basis for the invariant Compton amplitude is not unique [3], the basis in Eq.(2.2) is the most convenient for evaluating polarizabilities. Here, in Eq.(2.2), the structure functions R_i are directly related to the electric, magnetic and spin-dependent polarizabilities in the multipole expansion. If we keep only dipole-dipole and dipole-quadrupole transitions in the multipole expansion of the Compton structure functions [7], we have rather simple connecting formulas to the polarizabilities of the baryon:

$$\begin{gathered}R_1^{NB} = \omega^2\alpha_{E1};\;\; R_2^{NB} = \omega^2\beta_{M1};\;\; R_3^{NB} = \omega^3(-\gamma_{E1E1} + \gamma_{E1M2});\\ R_4^{NB} = \omega^3(-\gamma_{M1M1} + \gamma_{M1E2});\;\; R_5^{NB} = -\omega^3\gamma_{M1E2};\;\; R_5^{NB} = -\omega^3\gamma_{E1M2}.\end{gathered} \tag{2.3}$$

Although the polarizabilities used in Eq.(2.3) are defined as constants, it is essential to treat them as energy-dependent quantities [4]. The reason behind this extension to the dynamical (energy-dependent) polarizabilities is dictated by the fact that the Compton scattering experiments were performed with 50 to 800 MeV photons and hence required additional theoretical information to extrapolate the results to zero-energy parameters. It is also well known that the polarizabilities can become energy-dependent due to the internal relaxation mechanisms, resonances, and particle production thresholds. Accordingly, we keep all orders in ω for the Compton structure functions (for static polarizabilities we keep only order up to $\mathcal{O}(\omega^2)$ for $R_{1,2}$ and up to $\mathcal{O}(\omega^3)$ for $R_{3,4,5,6}$), and thus determine the energy-dependent polarizabilities. A connection between dynamic and static polarizabilities can be achieved by taking a limit to zero photon energy. The Compton structure functions up to one-loop order are calculated using CHM [5] based on the relativistic chiral perturbation theory. In addition, the structure-dependent pole contribution to the nucleon polarizabilities is taken into account in the form of the nucleon Δ-resonance excitation.

3. Results

The polarizabilities calculated for the proton with the photon energies up to 300 MeV are

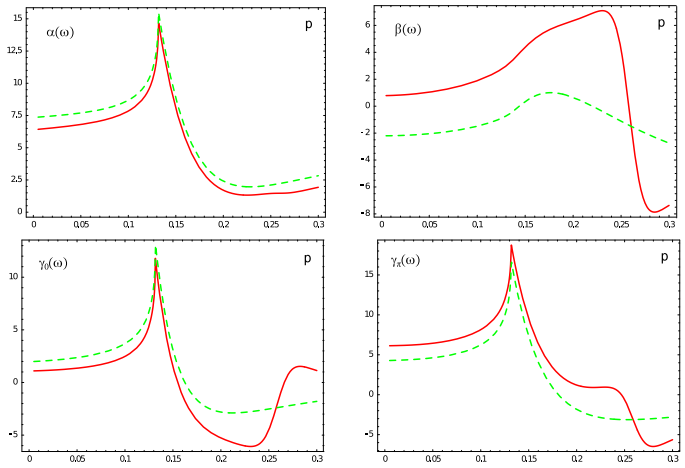

Figure 1: Dependencies of the proton electric, magnetic and spin-dependent polarizabilities on photon energy ω(GeV) in the center-of-mass reference frame. The first row (from left) corresponds to the electric and magnetic polarizabilities in $10^{-4}\,(fm^3)$. The second row are spin-dependent forward γ_0 and backward γ_π polarizabilities in $10^{-4}\,(fm^4)$. Green-dashed curve corresponds to the meson-nucleon loops contribution only and solid-red curve is the result with Δ resonance pole contribution added.

shown on Fig.1. It is evident that below 50 MeV they have very small energy dependence. For the neutron, the energy dependencies of the dynamical polarizabilities have similar behavior except the values are bigger on absolute scale. Here we will only provide a description for the proton dynamical polarizabilities.

The electric polarizability of the proton has very strong, resonance-type dependence near the pion production threshold. The Δ-pole contribution has a small effect while consistently reducing $\alpha_p(\omega)$ values for all the energies. Of course, to make final predictions in the ChPTh of the values of polarizabilities, it is required to add the contribution from the resonances in the Compton scattering loops. Hence, in order to compare our results with experimental values, we have used resonance loops results borrowed from the small scale expansion (SSE) approach [6]. If no Δ-pole contribution is added, the magnetic polarizability in Fig.1 stays negative (diamagnetic) for almost all the energies. The Δ-pole contribution is very large and shifts $\beta_p(\omega)$ from negative to positive (paramagnetic) values for energies up to 250 MeV. This behavior is quite natural, since the pion loop calculations reflect magnetic polarizability coming from the virtual diamagnetic pion cloud and the Δ resonance contribution to $\beta_p(\omega)$ is driven by the strong paramagnetic core of the nucleon. The spin-dependent polarizabilities, γ_0 and γ_π, have strong dependence near the pion production threshold and the Δ- pole contribution is evident near the Δ production threshold. If we take contributions of order $\mathcal{O}(p^3)$ in ChPTh power counting, we get an excellent agreement with [8]. Our result for the proton polarizabilities up to the one-loop order, plus including Δ- pole and SSE contribution is the following (in units of $10^{-4}(fm^3)$):

$$\alpha_p = (7.38\,(\pi-\text{loop}) - 0.95\,(\Delta-\text{pole}) + 4.2\,(\text{SSE})) = 10.63;$$
$$\beta_p = (-2.20\,(\pi-\text{loop}) + 3.0\,(\Delta-\text{pole}) + 0.7\,(\text{SSE})) = 1.49.$$

In the following table, we list the results for the spin-dependent static polarizabilities:

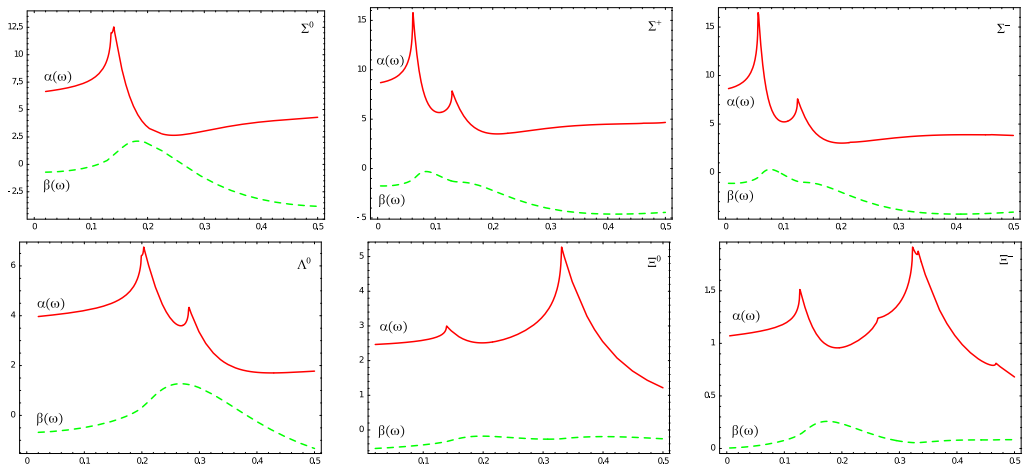

Figure 2: Electric and magnetic dynamical polarizabilities of hyperons in units of $10^{-4}\,(fm^3)$ as a function of the photon energy ω(GeV). Here, solid red line represents the electric polarizability and dashed green line is the magnetic polarizability.

$10^{-4}\,(fm^4)$	$\mathcal{O}(p^3)$[9]	$\mathcal{O}(p^4)$[10]	$\mathcal{O}(\varepsilon^3)$[11]	HYP. Dr. [12]	This work	Exp.
$\gamma_{0(p)}$	4.6	-3.9	2.0	-1.1	1.1	-0.90 ±0.08 ±0.11
$\gamma_{\pi(p)}$	4.6	6.3	6.8	7.8	6.1	8.0 ±1.8

The listed results have a broad spectrum of values, so clearly more work is needed in this area. Our values in this table do not include the Δ resonance in the loops, but if we follow the trend of the Δ- pole contribution into γ_0 and γ_π, we can see that inclusion of resonance in the loops for the Compton scattering will bring our results closer to the experimental values. The static electric and magnetic polarizabilities for hyperons have been first calculated in [13] and just recently calculations have been completed for the spin-dependent static polarizabilities in [14]. Both groups were using heavy baryon chiral perturbation theory. The dynamical electric and magnetic polarizabilities for hyperons first have been calculated in [15]. In Fig.2 we provide updated results for dynamical electric and magnetic polarizabilities for hyperons using basis from Eq.(2.2) in the Compton scattering amplitude.

For all polarizabilities listed in Fig.(2), the electric polarizabilities have very similar resonant-type behavior near the meson-production thresholds and the magnetic polarizabilities for all hyperons have negative low energy (static) values. Once again it is important to include both pole and loop resonance contributions for a complete analysis. In Fig.(3), we present the first results on the forward and backward spin-dependent dynamical polarizabilities for the hyperons.

As one can see from Fig.(3), for all hyperons, the spin-dependent backward polarizability dominates the forward polarizability on the absolute scale. Simultaneously, they all exhibit almost static behavior in the very low energy region of the Compton scattering. For all dynamical polarizabilities of the SU(3) octet of baryons, we find that their values are strongly governed by the excitation mechanism reflected in the meson production peaks. Hence the study of these polarizabilities directly probes the internal degrees of freedom which govern the structure of baryons at low energy. In this work, we have calculated the electric, magnetic and spin-dependent dynami-

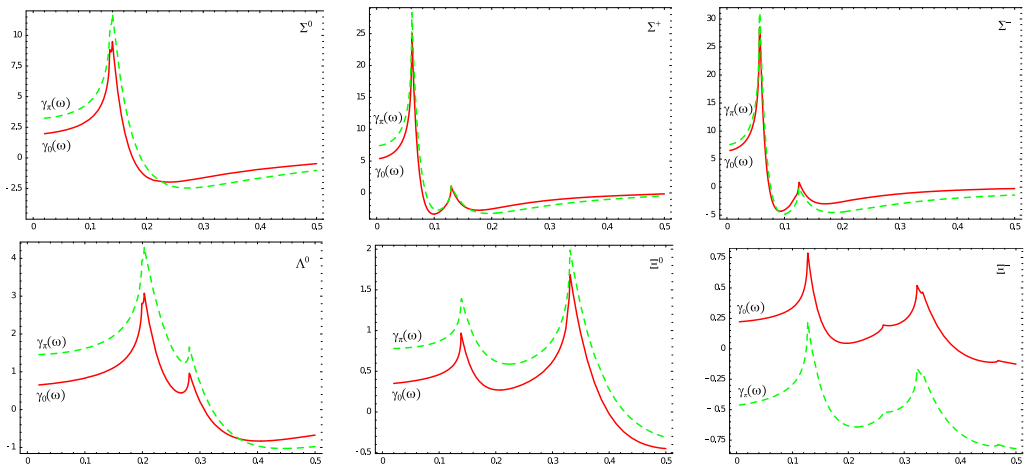

Figure 3: Forward (γ_0) and backward (γ_π) spin-dependent dynamical polarizabilities of hyperons in units of $10^{-4}\,(fm^4)$. Red solid line shows the forward spin-dependent polarizability and green dashed line corresponds to the backward spin-dependent polarizability.

cal polarizabilities of the SU(3) octet of baryons using ChPTh implemented in CHM. We found that predictions of the chiral theory derived from our calculations (up to one-loop order and not including resonances in loop calculations) are somewhat consistent with the experimental results. The calculations of the dynamical polarizabilities with baryon resonances in the loops is our current goal. It is also evident that further experimental work is needed, especially for the hyperon polarizabilities.

References

[1] J. Beringer et al. (Particle Data Group), Phys. Rev. D86, 010001 (2012).

[2] B. Pasquini, D. Drechsel, and M. Vanderhaeghen, Eur. Phys. J. Special Topics 198, 269–285 (2011).

[3] D. Babusci, G. Giordano, A.I. L'vov , G. Matone, A.M. Nathan, Phys.Rev. C58 (1998) 1013-1041

[4] R. P. Hildebrandt, H. W. Griesshammer, T. R. Hemmert, B. Pasquini, Eur. Phys. J A 20, 293-315 (2004).

[5] A. Aleksejevs, M. Butler, J.Phys. G37 (2010) 035002

[6] T. R. Hemmert, B. R. Holstein, J. Kambor, Phys. Rev. D 55, 5598 (1997).

[7] V.I. Ritus, ZhETP 32, 1536 (1957) [Sov. Phys. JETP 5, 1249 (1957)].

[8] Lensky & Pascalutsa Eur.Phys.J.C65:195-209, (2010).

[9] T. R. Hemmert, B. R. Holstein, J. Kambor and G. Knochlein, Phys. Rev. D 57, (1998) 5746.

[10] K. B. Vijaya Kumar, J. A. McGovern and M. C. Birse, Phys. Lett. B 479, (2000) 167.

[11] G. C. Gellas, T. R. Hemmert and U. G. Meissner, Phys. Rev. Lett. 86, (2001) 3205.

[12] D. Drechsel, B. Pasquini and M. Vanderhaeghen, Phys. Rept. 378, (2003) 99.

[13] V. Bernard, N. Kaiser, J. Kambor and U. Meissner, Phys. Rev. D 46, 7 (1992).

[14] K.B. Kumar, A. Faessler, T. Gutsche, B. Holstein, V. Lyubovitskij, Phys.Rev. D84, 076007 (2011).

[15] A. Aleksejevs and S. Barkanova, J.Phys. G38 (2011) 035004